Fate and Plasticity of the Epidermis in Response to Congenital Activation of BRAF

Suguna R. Krishnaswami[1], Shantanu Kumar[1], Phillip Ordoukhanian[2] and Benjamin D. Yu[1]

Germline and somatic mutations in RAS and its downstream effectors are found in several congenital conditions affecting the skin. Here we demonstrate that activation of BRAF in the embryonic mouse ectoderm triggers both craniofacial and skin defects, including hyperproliferation, loss of spinous and granular keratinocyte differentiation, and cleft palate. RNA sequencing of the epidermis confirmed these findings but unexpectedly revealed evidence of continued epidermal maturation, expression of >80% of epidermal differentiation complex genes, and formation of a hydrophobic barrier. Spinous and granular differentiation were restored by pharmacologic inhibition of MAPK/ERK kinase or BRAF. However, restoration of epidermal differentiation was non-cell autonomous and required dermal tissue to be present in tissue recombination studies. These studies indicate that early activation of the RAF signaling pathway in the ectoderm has effects on specific steps of epidermal differentiation, which may be amenable to treatment with currently available pharmacologic inhibitors.

Journal of Investigative Dermatology (2015) **135,** 481–489; doi:10.1038/jid.2014.388; published online 30 October 2014

INTRODUCTION

In addition to its well-known involvement in cancer, mutations in the RAS pathway can also be found as germline or early somatic mosaic mutations (Hafner and Groesser, 2013; Rauen, 2013). These early mutations occur in a spectrum of congenital diseases, which affect internal organ, skin and hair development, several types of neoplasms, and constitutional maturation. Understanding the pathogenesis and timing of these defects is critical to implementing the use of widely available RAS pathway inhibitors in the treatment of these children early in the course of disease.

The genetics of RAS/MAPK (mitogen-activated protein kinase)-associated diseases suggest that mutations trigger RAS paralog and effector-specific developmental and pathologic responses. HRAS mutations are far more common in the Costello syndrome than are KRAS mutations (95% *HRAS*; 5% *KRAS;* 0% *NRAS*) (Aoki *et al.*, 2008). Mutations in *BRAF* and *RAF1* are exclusively involved in the cardiofaciocutaneous syndrome (Rodriguez-Viciana *et al.*, 2006) and the Noonan syndrome (Razzaque *et al.*, 2007), respectively. Germline mutations in parallel RAS effector pathways, AKT/ PTEN, cause yet other distinct diseases (Liaw *et al.*, 1997; Pilarski *et al.*, 2013). Finally, early post-zygotic mutations also disproportionately involve specific RAS paralogs (*HRAS, KRAS*) and RAS effectors (*AKT1*) in diseases such as epidermal nevus, nevus sebaceous, Schimmelpennig, and Proteus syndromes (Lindhurst *et al.*, 2011; Groesser *et al.*, 2012; Levinsohn *et al.*, 2013).

The spectrum of skin disease in RAS/MAPK syndromes suggests that the ectoderm discriminates between mutations in specific effectors and paralogs. In the *HRAS*-associated Costello syndrome, children develop redundant skin folds and papillomas, whereas *BRAF/MEK* (MAPK/ERK kinase)-associated disease is associated with flaky skin (ichthyosis), perifollicular hyperkeratosis (keratosis pilaris), and lacks papillomas (Turnpenny *et al.*, 1992; Siegel *et al.*, 2011). *RAF1* mutations in the Noonan syndrome children trigger neither of the above cutaneous features (Roberts *et al.*, 2006). The mechanisms that are responsible for differences in cutaneous responses to paralogs and downstream effectors of RAS are not known.

To study the effects of congenital BRAF activation of epidermal development, we used a knock-in model to activate BRAF ($Braf^{V600E}$) in the ectoderm during embryogenesis. BRAF activation induces hyperplasia and interferes with progressive differentiation of the embryonic epidermis, where intermediate steps in differentiation are lost. Through RNA sequencing, *in situ* hybridization and skin barrier assay, we find that maturation of the epidermis and barrier formation continues. Inhibitors of either MEK or BRAF rescue spinous and granular keratinocyte differentiation in explants of *K14*-cre; $Braf^{V600E}$ mice, demonstrating both plasticity and continued responsiveness of affected epidermis. These findings reveal that congenital activation of BRAF causes specific cell identity defects in epidermal development and provides insights into the mechanisms and application of BRAF/MEK inhibition in the treatment of skin disease.

[1]*Division of Dermatology, Department of Medicine, Institute for Genomic Medicine, Stem Cell Program, University of California, San Diego, La Jolla, California, USA and* [2]*Next Generation Sequencing Core, The Scripps Research Institute, San Diego, California, USA*

Correspondence: Benjamin Yu, UCSD School of Medicine, Division of Dermatology, 9500 Gilman Drive, MC-0869, La Jolla, California 92093-0869, USA. E-mail: byu@ucsd.edu or mail.benjaminyu@gmail.com

Abbreviations: FLG, filaggrin; LOR, loricrin; MAPK, mitogen-activated protein kinase; MEK, MAPK/ERK kinase

Received 19 March 2014; revised 7 August 2014; accepted 19 August 2014; accepted article preview online 9 September 2014; published online 30 October 2014

RESULTS

Congenital activation of BRAF in the embryonic ectoderm

To activate BRAF in the ectoderm, we utilized a mouse model, where expression of a mutant allele (*Braf*^{V600E}) remains under the control of its endogenous locus and produces mutant product following Cre-mediated deletion of a transcription stop cassette (Dankort *et al.*, 2007). *Braf*^{V600E} floxed females were bred to *Keratin 14* (*K14*)-cre) transgenic males, which express *Cre* in the epidermis at embryonic day (E) 14.5 (Vasioukhin *et al.*, 1999). *K14*-cre-positive, *Braf*^{V600E}-positive (*K14*-cre; *Braf*^{V600E}) offspring were produced at near expected Mendelian frequency when assessed prior to birth (25.6% observed; 25% expected from 167 late stage embryos). Postnatally, the majority of *K14*-cre; *Braf*^{V600E} newborns were cannibalized by adults, and only three *K14*-cre; *Braf*^{V600E} mice out of >20 litters were detected at the time of weaning. In litters observed at the moment of birth, *K14*-cre; *Braf*^{V600E} newborns showed severe ectodermal defects, including thick, fissured scale overlying translucent edematous skin, and displayed rhythmic ventilation and pink oxygenation. Further examination of *K14*-cre; *Braf*^{V600E} newborns also revealed lack of ingested milk in their stomachs and cleft palate defects in >84% (Figure 1b). The latter defect may result from Cre expression in the palate epithelium of K14-cre animals (Okubo *et al.*, 2009). Histologic analysis of the skin revealed a thickened epidermis, basaloid cells, cytolysis, and loss of keratohyalin granules (Figure 1c). Although a stratified epithelium was present in *K14*-cre; *Braf*^{V600E} mice, immunofluorescent analysis revealed loss of K10-positive spinous and loricrin/filaggrin (LOR/FLG)-positive granular keratinocytes (Figure 1c). The *K14*-cre; *Braf*^{V600E} epidermis was hyperproliferative as evidenced by increased BrdU-staining and the overexpression of K6 protein.

Congenital BRAF activation does not prevent continued differentiation

To characterize the differentiation and fate of the *K14*-cre; *Braf*^{V600E} epidermis, high-throughput sequencing of transcripts was performed from the E17.5 epidermis, when the skin was phenotypically abnormal but lacked extensive signs of cytolysis seen at later stages. Pooled total RNA from four control littermate and mutant E17.5 epidermis was used to generate 48.4 and 56.3 million read libraries, respectively, and unique reads were aligned to the genome and annotated (Figure 2). A total of 2,189 coding genes were differentially expressed in the *K14*-cre; *Braf*^{V600E} epidermis, many of which participate in epidermal differentiation and keratinization (Figure 2a). Because of the heterogeneity of epidermal tissue, gene expression data may also reflect the presence of other cell types and follicular tissues. These data were used to study the activity of genes representing specific epidermal lineages (Figure 2b; Supplementary Figure S1 online), including late steps in differentiation, which involve activation of >70 epidermal differentiation complex genes (de Guzman Strong *et al.*, 2010). Read coverage within the 3.3 Mb interval of conserved gene cluster was analyzed and identified 63 transcriptional units, which are located in five physical groups (Figure 2c). Loss of gene expression was most prominent in the LCE-like group III, where the majority of these genes were decreased by twofold except for four outliers in this group representing *Lce3* paralogs, which were upregulated (Figure 2d). In the remaining epidermal differentiation complex groups, >85% (41 genes) were expressed at normal or higher levels in *K14*-cre; *Braf*^{V600E} epidermis (Supplementary Figure S2 online). These findings reveal that despite the loss of early and intermediate gene differentiation, the vast majority of transcriptional features of late differentiation remain active.

To confirm transcriptional changes identified by RNA-seq of pooled samples, real-time quantitative PCR for select differentiation markers was performed on individual embryos (Figure 3 and Supplementary Table S1 online). *K14*-cre; *Braf*^{V600E} consistently demonstrated high levels of basal lineage gene expression (*K5*, *K14*), whereas spinous (*K1*, *K10*) and granular (*Lor*, *Flg*)-specific gene expression was markedly reduced (Figure 3b). Late epidermal differentiation genes, *Lce3b*, *Lce3c*, *S100a1*, *S100a10*, and *Sprr2i*, were still expressed in the *K14*-cre; *Braf*^{V600E} embryos and in some cases at higher levels than in wild-type littermates.

To identify the pattern of differentiation in *K14*-cre; *Braf*^{V600E} epidermis, RNA *in situ* hybridization was performed (Figure 3c). The patterns of early, intermediate, and late terminal differentiation gene expression in wild type and *K14*-cre; *Braf*^{V600E} embryos demonstrated that late terminal differentiation gene expression remains restricted to the most distal layers. Localization of gene expression was further confirmed by tyramide-based detection, which produces a nondiffusible signal (Supplementary Figure S3 online). Thus, a spatial or temporal mechanism persists in the *K14*-cre; *Braf*^{V600E} epidermis allowing for layer-specific gene expression in the upper epidermis.

Terminal steps in epidermal differentiation are critical for generating a hydrophobic barrier. This barrier becomes evident between E16.5 and E17.5 and can be detected by exclusion of water-soluble dyes, such as toludidine blue (Hardman *et al.*, 1998). Between E14.5 and E17.5 (Supplementary Figure S4 online.), *K14*-cre; *Braf*^{V600E} embryos appeared opaque relative to littermates at E16.5 and showed widespread hyperkeratosis at E17.5 (Supplementary Figure S4a online). Cornified sheets from *K14*-cre; *Braf*^{V600E} embryos at E18.5 were more brittle compared to wild-type littermates (Supplementary Figure S4b online). At E16.5, partial dye exclusion was visible in wild-type littermates (light blue) in the dorsal skin (Supplementary Figure S4b online). A similar dorsal pattern of dye exclusion was present in *K14*-cre; *Braf*^{V600E} embryos, but dye exclusion was more complete resulting in its white appearance. By E17.5 and just prior to birth, wild type and *K14*-cre; *Braf*^{V600E} embryos demonstrated similar patterns of barrier dye staining. Thus, in the presence of *Braf*^{V600E}, the epidermis is still capable of producing a hydrophobic barrier.

Plasticity and requirements for layer identity in response to BRAF and MEK inhibition

Pharmacologic inhibition of c-RAF, BRAF, and MEK1/2 is a major focus in cancer drug discovery and may be a source for potential therapies in rare childhood disorders. To explore this

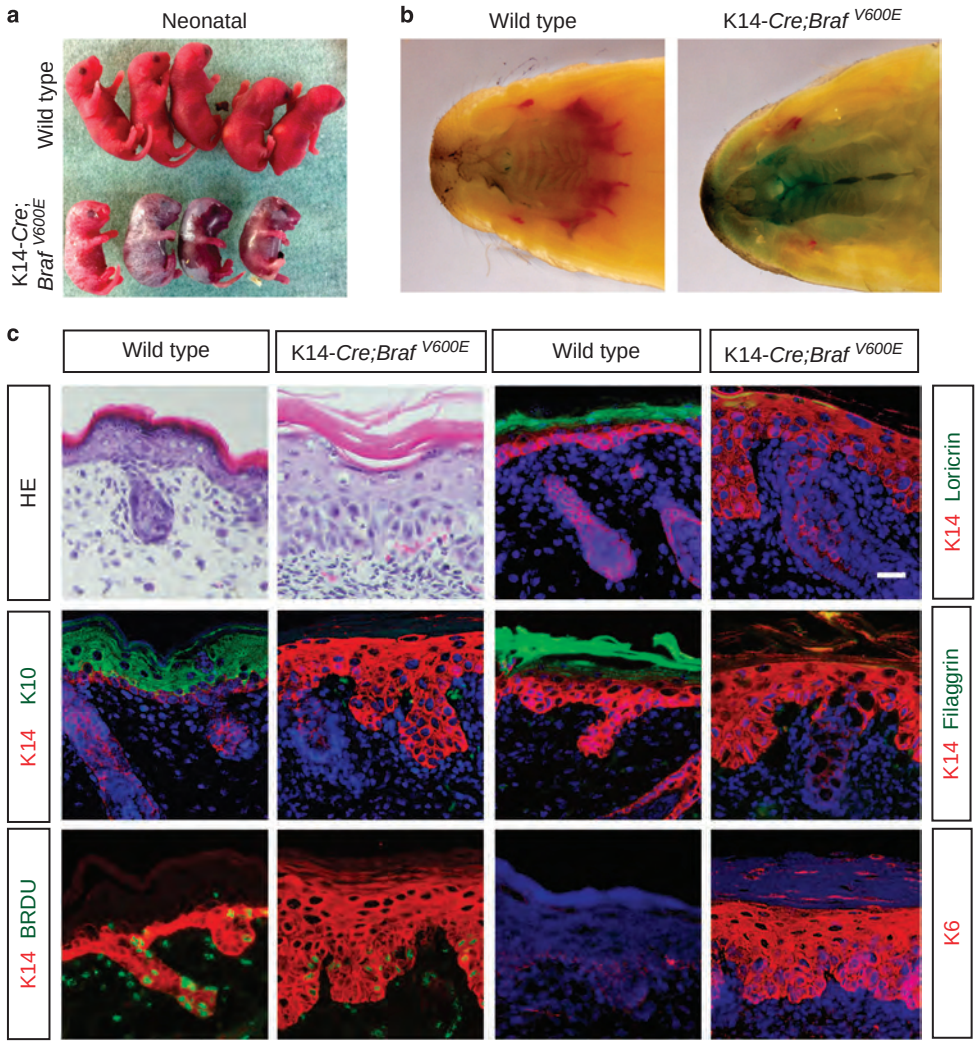

Figure 1. Phenotype of *K14*-cre; *Braf*^{V600E} neonatal and perinatal mice. (**a**) Appearance of normal neonatal (upper row) and *K14*-cre; *Braf*^{V600E} (bottom row) littermates. The *K14*-cre; *Braf*^{V600E} skin appeared flaky and fissured overlying areas of translucent skin. (**b**) Cleft palate defects in *K14*-cre; *Braf*^{V600E} whole mount preparations were counterstained with toluidine blue. (**c**) Histologic and immunofluorescent analysis of *K14*-cre; *Braf*^{V600E} (*Braf*^{V600E}) neonatal skin. Hematoxylin and eosin (HE)-stained sections demonstrate thickened epidermis, separation of individual cells, and severe reduction in cytoplasmic keratohyalin granules. Immunofluorescent staining for K10, BrdU, loricrin (LOR), filaggrin (FLG), and K6 is shown for perinatal wild-type littermate and *K14*-cre; *Braf*^{V600E} E18.5-P0 mouse skin. Note the absence of K10-positive-spinous keratinocytes and LOR/FLG-positive granular keratinocytes in the *K14*-cre; *Braf*^{V600E} mouse skin. K6, a marker for hyperproliferative skin, is increased in the *K14*-cre; *Braf*^{V600E} mouse skin. Scale bars=20 μm.

possibility, mouse embryonic explants containing E17.5-E18.5 skin biopsies were cultured for 24 hours in the presence of inhibitors of BRAF or MEK1/2 (Figure 4). PLX4720 is selective inhibitor of BRAF with a 10-fold higher affinity for BRAF^{V600E} than for wild-type BRAF (Tsai *et al.*, 2008; Bollag *et al.*, 2010). Paradoxically, low doses of PLX4720 (<1 μM) lead to compensatory activation of c-RAF and MEK1/2 and proliferation, resulting in increased keratoacanthomas and squamous cell carcinomas (Chapman *et al.*, 2011). As a result, high doses (>10 μM) of PLX4720 and other BRAF inhibitors are used to suppress RAF paralogs and MEK (Poulikakos *et al.*, 2010).

To assess BRAF inhibition in small amounts of explanted tissues, we assessed expression of a downstream target gene, *Dusp6*, which is induced by RAS/MAPK signaling. *Dusp6* was elevated in K14-*cre*; *Braf*^{V600E} epidermis and downregulated in the presence of high-dose (>50 μM) PLX4720 (Figure 4a, left panel) (Bloethner *et al.*, 2005). We next assessed early differentiation in response to BRAF inhibition (Figure 4a, right panel) and found increased *K1*, *K10*, and *Lor* expression in K14-*cre*; *Braf*^{V600E} epidermis ($P=0.006$) and in wild-type littermate epidermis.

To confirm that inhibition of BRAF and downstream effectors, MEK1/2, are responsible for the reversal of the K14-*cre*; *Braf*^{V600E} phenotype, we also treated explants with U0126, which is a noncompetitive inhibitor of MEK1 and MEK2 (Sebolt-Leopold, 2008). MEK inhibition resulted in decreased *Dusp6* (Mukhopadhyay *et al.*, 2012), and

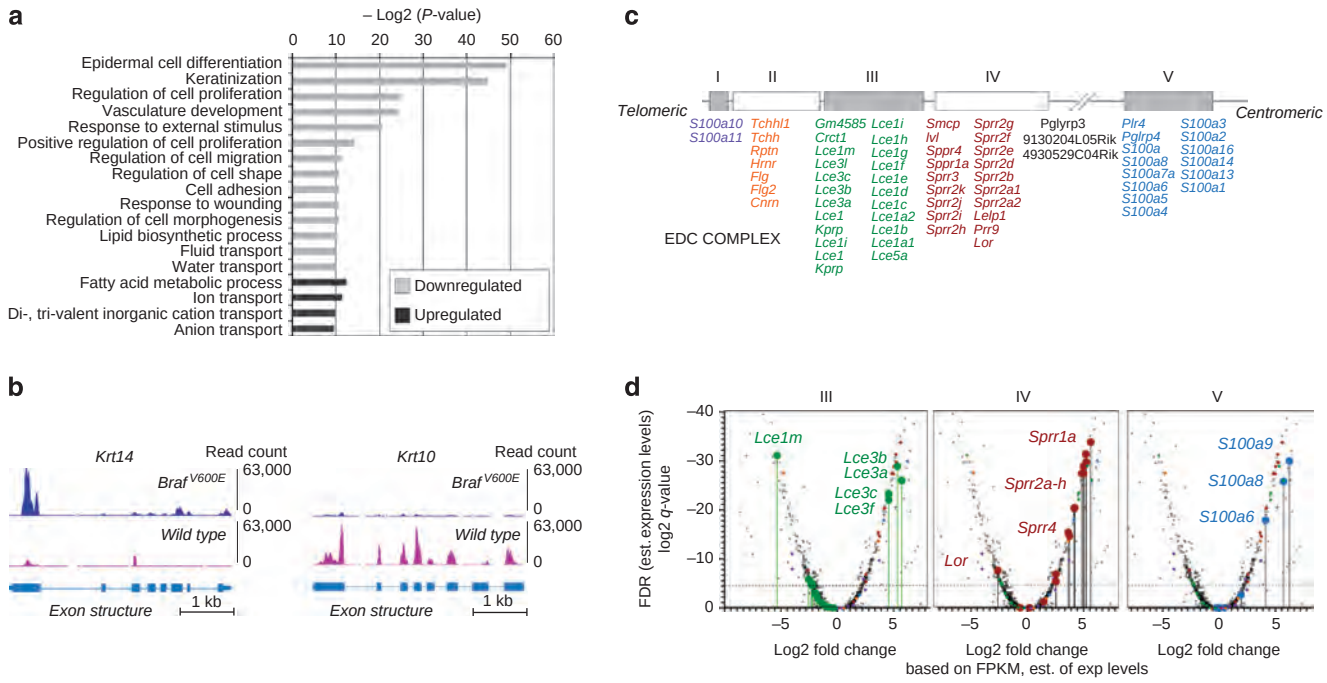

Figure 2. RNA sequencing identifies the fate of epidermis in *Braf*^{V600E} mutant mice and persistence of EDC gene expression. (**a**) Functional classification of genes differentially expressed in E17.5 *K14*-cre; *Braf*^{V600E} epidermis demonstrating number of genes and statistical significance of their association. (**b**) Read coverage of wild type vs. *K14*-cre; *Braf*^{V600E} transcripts across the mouse *Krt14* and *Krt10* loci. (**c**) Intermediate and late differentiation genes clustered in the EDC locus and close proximity of closely related paralogs. (**d**) Volcano plots of relative expression of all EDC group genes from pooled wild type vs. *K14*-cre; *Braf*^{V600E} embryos. Specific groups of EDC genes, LCE-like (green), SPRR-like (red), and S100 family genes (blue), are colored and shown as balloons in respective cluster III, IV, and V. The levels of gene expression in RNA-seq are estimated from (**b**) and have associated $\log_2$ *q*-values or false discovery rates (vertical axis) for this estimate. Note: this *q*-value does not reflect sample variance, as specimens have been pooled.

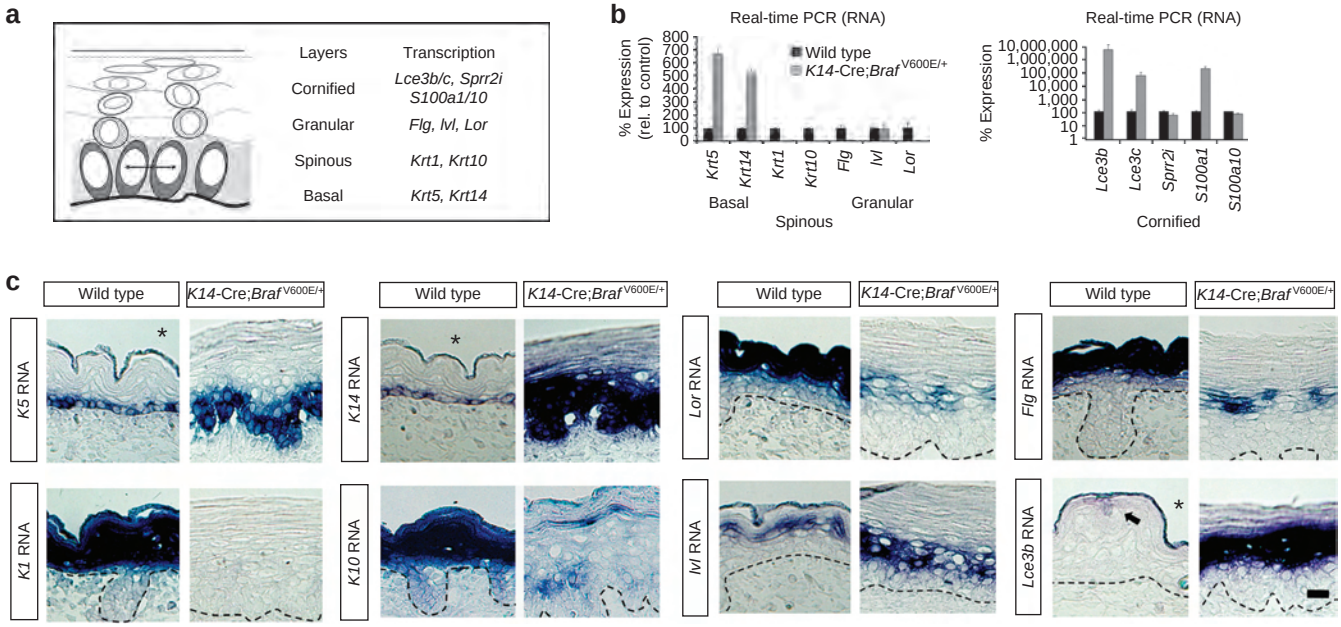

Figure 3. Expression of intermediate and late stage epidermal differentiation genes in *K14*-cre; *Braf*^{V600E} mice. (**a**) Differentiation markers used to identify basal (SB), spinous (SS), granular (SG), and cornified envelope (SC) keratinocytes. (**b**) Real-time PCR for gene expression at E17.5 skin reveals loss of spinous and granular differentiation markers in *K14*-cre; *Braf*^{V600E} embryos and the presence of late differentiation markers (*Lce3b, Lce3c, Sprr2i, S100a1, and S100a10*). Error bars represent SD of four animals of each genotype. (**c**) E17.5 i*n situ* hybridization of basal *K5*/*K14*, spinous *K1*/*K10*, granular *Lor*/*Flg*, involucrin, and cornified envelope *Lce3b* keratinocyte gene expression. These studies show the loss of spinous and granular keratinocyte gene expression and pattern of involucrin and cornified envelope genes in upper layers. Supplementary Figure S3 online further localizes gene expression by tyramide signal amplification. Scale bars=20 μm.

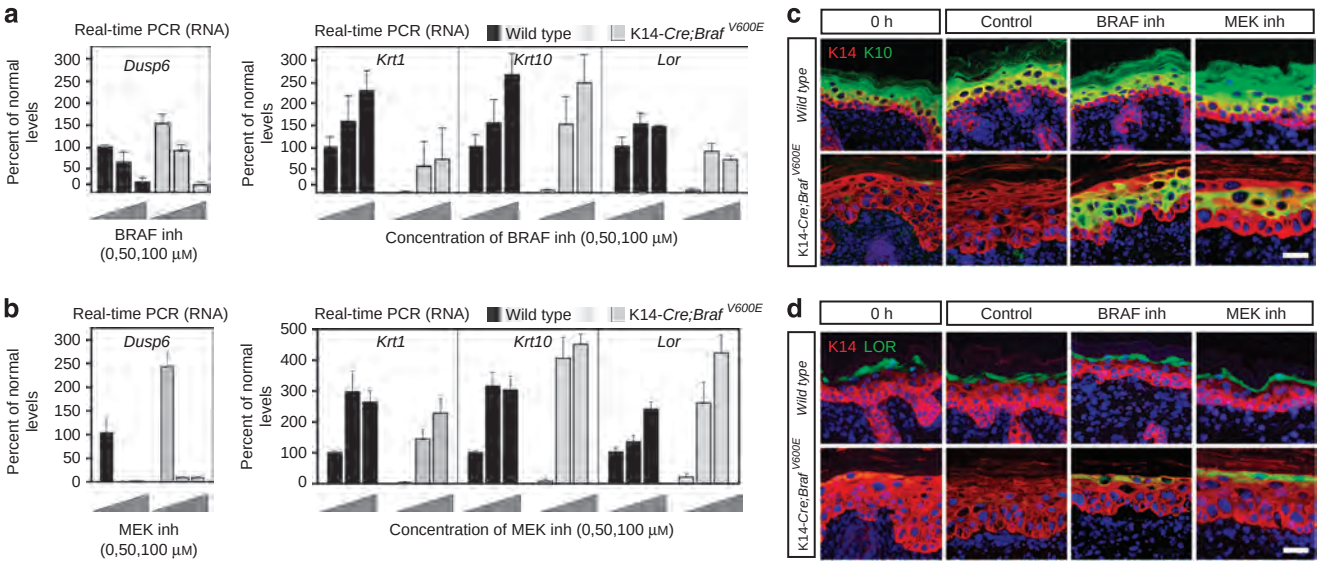

Figure 4. Rescue of spinous and granular keratinocyte expression by pharmacologic inhibition of BRAF or MEK. Wild type and K14-cre; *Braf*^{V600E} explants were treated with PLX4720, U0126, or vehicle for 24 hours. (**a**) Real-time qPCR of *Dusp6*, a transcriptional target of RAS/MAPK signaling, and differentiation markers (*Krt1*, *Krt10*, and *Lor*) in E17.5 skin after treatment with varying doses of PLX4720. (**b**) Real-time PCR of *Dusp6*, *Krt1*, *Krt10*, and *Lor* gene expression in wild type and *K14*-cre; *Braf*^{V600E} skin explants with U0126. (**c**, **d**) Immunostaining of (**c**) K10 and K14 or (**d**) LOR and K14 prior to culture and after culture in vehicle, 100 μM PLX4720, or U0126. Error bars represent SD of a minimum of three samples for each condition. Scale bars=20 μm.

reactivation of spinous and granular layer gene expression (*K1, K10, Lor*) (Figure 4b) and partial correction of other genes (Supplementary Figure S7 online). These studies indicated that continuous BRAF activity via MEK activation is necessary for skin defects and that plasticity remains in the *K14*-cre; *Braf*^{V600E} mice. To identify which layers of the epidermis respond to BRAF/MEK inhibition, we performed immunofluorescent and *in situ* hybridization studies on PLX4720-treated explants (Figure 4 and not shown). PLX4720 and U0126 restored K10-positive staining of cells in layer number 2 through 4 of *K14*-cre; *Braf*^{V600E} explants but did not activate K10 in more distal layers. In contrast, the distal layers of the wild-type epidermis express both K10 and granular layer proteins—e.g., LOR. In *K14*-cre; *Braf*^{V600E} mice, this distal layer is, however, able to respond to BRAF or MEK inhibition in its expression of LOR (Figure 4).

Plasticity in the above studies could arise from basal keratinocytes responding to BRAF inhibition or keratinocytes already residing in distal layers. To label these populations, we performed a pulse-chase labeling to follow the fate of proliferating basal keratinocytes after BRAF inhibition (Figure 5 and Supplementary Figure S8 online). BrdU was introduced *in utero* to pregnant females, and embryos and skin explants were isolated 2 hours later to identify pulse-labeled cells. In *K14*-cre; *Braf*^{V600E} explants, 47.3 ± 4.4% of basal keratinocytes vs. 29.8 ± 4.7% in wild-type basal keratinocytes were BrdU-labeled at $t = 2$ hours (Figure 5a). After a 24-hour chase in BrdU-free culture, we found that the majority of K10- and LOR-positive keratinocytes in PLX4720-treated explants do not arise from label-retaining keratinocytes cells. These observations suggest that PLX4720 inhibition triggers *K10* and *Lor* gene expression in post-mitotic layers.

Non-cell autonomous requirements of *Braf*^{V600E} explants

The persistence of spatial patterning in *K14*-cre; *Braf*^{V600E} epidermis suggested that spinous and granular cell identities may still be silently present in the epidermis, despite their lack of layer-specific gene expression. To test for the continued presence of ''silent'' spinous and granular layer identity, we studied whether the keratinocyte response to BRAF inhibition was cell-autonomous. Using dissociated keratinocytes from *K14*-cre; *Braf*^{V600E} embryos, cells were treated with BRAF inhibitor for 24 hours and tested for K10 and LOR reactivation (Supplementary Figure. S5 online). Under these conditions, neither K10 nor LOR expression was reactivated even though cells remain transcriptionally active. These observations suggest that reemergence of spinous and granular layer identity in the *K14*-cre; *Braf*^{V600E} epidermis is not a cell-autonomous process.

Because reactivation of spinous and granular keratinocyte identities failed to occur in dissociated cells, we further tested whether surrounding tissues contribute to the epidermal response to BRAF inhibition. Previous tissue recombination studies suggest an important role for the dermis in the histogenesis of the epidermis (Sengel, 1976). Therefore, we removed the dermis and tested the response of epidermal sheets from wild type and *K14*-cre; *Braf*^{V600E} mouse embryos to PLX4720 (Figure 6). In the absence of the dermis, neither K10 nor LOR expression was restored by PLX4720 (Figure 6a and b). As a control, we also tested the response of epidermal sheets after reattachment to the dermis (Figure 6a and b). Reattachment of the epidermis to the dermis restored the capacity of the epidermis to respond to BRAF inhibition and demonstrates the dermis directly or indirectly provides cues

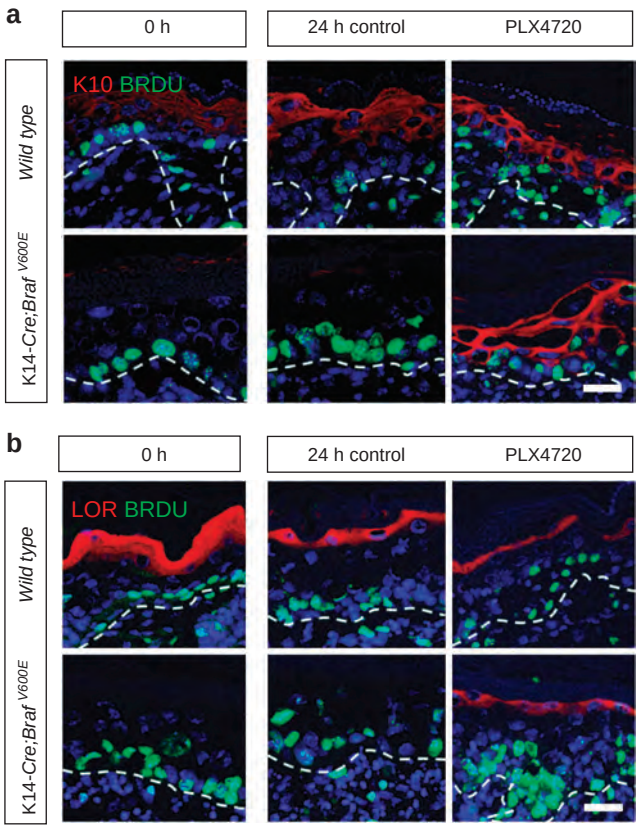

Figure 5. Fate of pulse-labeled basal keratinocytes in wild-type and *Braf*^{V600E} explants. To determine the origin of spinous and granular layer revertants in wild-type and *Braf*^{V600E} explants, proliferating basal keratinocytes were labeled *in utero* with BrdU, and after embryo harvest and explant culture for 24 hours in the presence of vehicle or PLX4720, BrdU was localized. (**a**) Double staining for K10 and pulse-chase BrdU demonstrates the labeling at time 0 hours and retention in post-mitotic cells 24 hours after vehicle vs. PLX4720 treatment. (**b**) Double staining for loricrin and pulse-chase BrdU demonstrates lack of BrdU-labeled cells in loricrin-positive cells. In all panels, dotted lines indicate epidermal junction with the dermis. Scale bars=20 μm.

necessary for specification of spinous and granular keratinocyte identity.

DISCUSSION

Epidermal differentiation is thought to occur in a linear manner during the formation of the stratified layers in the skin. Progressive pattern of differentiation is seen in other tissues, including early embryogenesis, hematopoiesis, neurogenesis, T- and B-cell selection, and elsewhere (Morrison *et al.*, 1997; Lanzavecchia and Sallusto, 2002). On the basis of RNA expression profiling of the *K14*-cre; *Braf*^{V600E} mice, we show that skin development may be less restrictive compared to other models of progressive differentiation (Caplan and Ordahl, 1978; MacLean, 1987).

Evidence from previous studies suggests that the intermediate stages of epidermal differentiation can have alternative identities. During embryogenesis, a transient population of K10^{pos} suprabasal keratinocytes, known as the stratum intermedium, continues to display proliferative potential (Sengel, 1976; Koster and Roop, 2007). In addition, changes in keratinocyte identity and potential have been noted after engraftment (Mannik *et al.*, 2010). Further evidence of alternative keratinocyte identities has also been observed in the postnatal tail epidermis, where alternating patterns of K10 expression are observed in suprabasal scale and interscale keratinocytes (Gomez *et al.*, 2013). These examples and the results of the *K14*-cre; *Braf*^{V600E} mouse indicate that spinous and granular keratinocyte differentiation may not be a required step in epidermal differentiation.

The loss of a cell type or stage presents a common dilemma in stem cell biology, where loss of lineage markers may signify either a change in cell identity or a more limited change—e.g., downregulation of specific markers (Spivakov and Fisher, 2007). To determine whether a ''silent'' spinous and granular keratinocyte cell identity persist in BRAF-activated keratinocytes, we tested the cell autonomy of the BRAF/MEK inhibitor response. In both assays, isolated keratinocytes and epidermal sheets, BRAF and MEK inhibition failed to rescue spinous and granular keratinocyte gene expression. The results of these studies suggest that these particular cell types require additional signals to re-activate spinous and granular identities. Whether these cells adopt an alternative identity in the *K14*-cre; *Braf*^{V600E} mouse remains to be determined.

The *K14*-cre; *Braf*^{V600E} mouse model exhibits a model for epidermal hyperproliferation in addition to the absence of intermediate layers. The overexpression of RAF1-estrogen receptor fusion protein similarly displays basal hyperproliferation and impairs epidermal differentiation (Tarutani *et al.*, 2003). Hyperproliferation of the epidermis, however, is not always linked to a block in differentiation. For example, both overexpression of Transforming growth factor-alpha or conditional activation of *Kras*^{G12D} lead to hyperproliferation but do not block epidermal differentiation (Vassar and Fuchs, 1991; Mukhopadhyay *et al.*, 2011). Thus, the inhibitory effects of RAS/MAPK signaling may be more specific to BRAF or RAF activation. Mouse models of activated *Hras, Kras, Raf1,* and *Braf* have previously been reported. These mice surprisingly exhibit major differences in skin phenotypes and even lack of skin phenotypes (Tarutani *et al.*, 2003; Schuhmacher *et al.*, 2008; Chen *et al.*, 2009; Mukhopadhyay *et al.*, 2011; Urosevic *et al.*, 2011). A previously reported *Braf*^{V600E}/*Braf*^{V600E} germline mutation in mouse does not lead to major epidermal differentiation defects (Urosevic *et al.*, 2011). The knock-in targeting strategy used to generate the conditional *Braf*^{V600E} allele used in our study differs from the germline *Braf*^{V600E}/*Braf*^{V600E} mouse model, which expresses the mutant allele at different levels (80% of wild-type levels in the conditional *Braf*^{V600E} model vs. ~30% in the germline *Braf*^{V600E}/*Braf*^{V600E}) (Supplementary Figure S6 online). These differences in expression levels of *Braf*^{V600E} likely account for differences in skin phenotypes. Neither mouse model (*Braf*^{V600E} allele) completely recapitulates alleles found in human cardiofaciocutaneous syndrome; however, species differences such as the relative resistance of rodent models to RAS (Kakumoto *et al.*, 2006; Muto *et al.*, 2006) further complicate these comparisons.

Our findings may have medical relevance to the manipulation of the BRAF/MEK pathway in the treatment of several

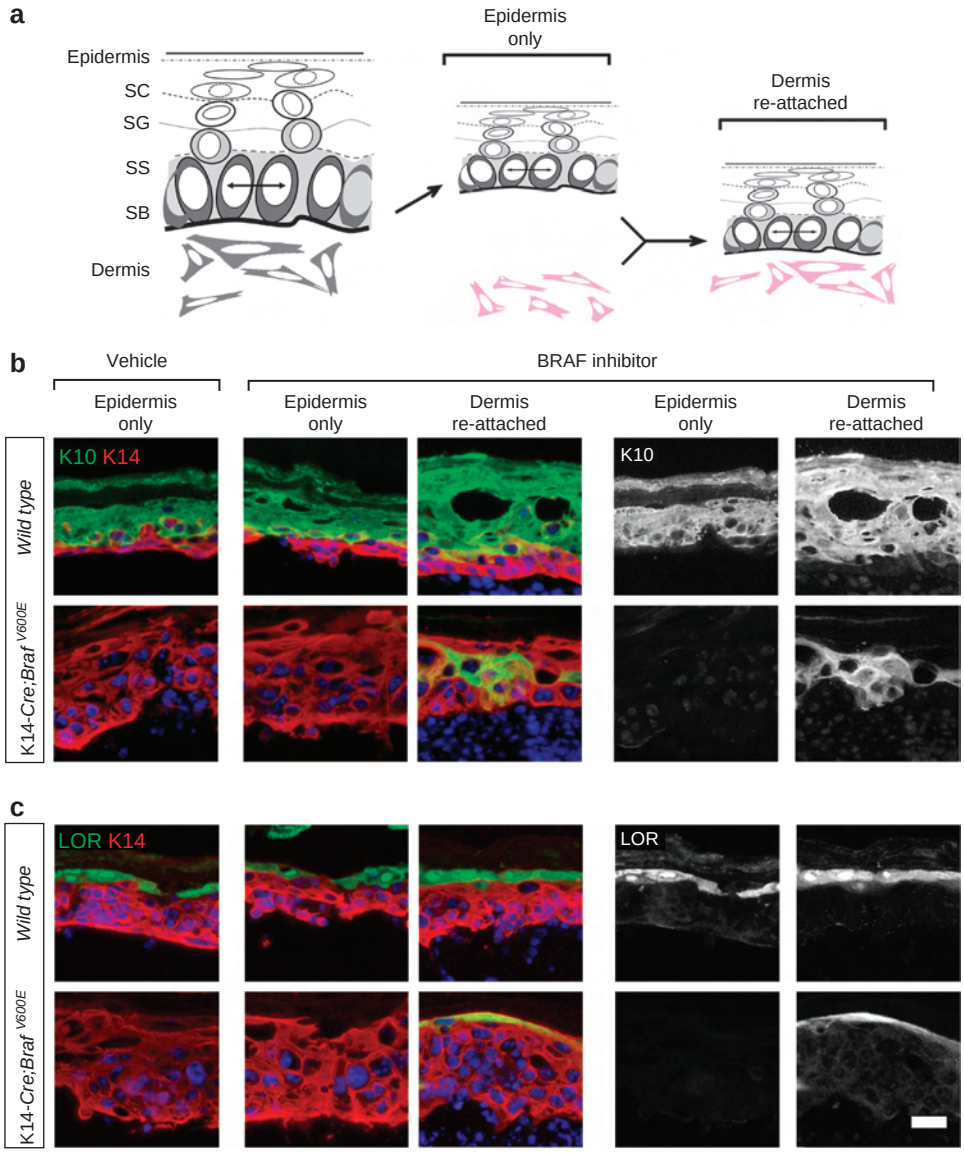

Figure 6. Reversion of *Braf*^{V600E} explants is not cell autonomous, requiring a dermal signal. (**a**) Schematic of preparation of explants, epidermis-only vs. epidermis with the dermis reattached. (**b**) Spinous K10 expression in epidermis-only explants vs. epidermis reattached to the dermis from wild type and *K14*-cre; *Braf*^{V600E} E17.5 embryos treated with BRAF inhibitor, PLX4720. Right panels demonstrate single channel of K10 expression. (**c**) Granular LOR expression was examined in wild-type and *Braf*^{V600E} epidermis, demonstrating the requirement for dermal reattachment for proper reactivation of LOR protein expression. Right panels demonstrate single channel of LOR expression. Scale bar=20 μm.

epidermal disorders. In the human skin, defects in intermediate stages of epidermal differentiation can be seen. In psoriasis, loss or reduction in granular keratinocyte differentiation has been observed (Chowaniec *et al.*, 1981). Similarly, in the wound response, spinous and granular keratinocyte markers are downregulated (Patel *et al.*, 2006; Ortonne *et al.*, 1981). In both settings, increased RAS/MAPK signaling has been reported (Sosnowski *et al.*, 1993; Lin *et al.*, 1999). Our findings support the model that RAS/MAPK signaling may be responsible for some aspects of these epidermal changes; however, further studies are needed to determine how human skin conditions respond to BRAF/MEK inhibition.

MATERIALS AND METHODS

Animal studies

Conditional *Braf*^{V600E} (Dankort *et al.*, 2007) and *K14*-cre mice (Vasioukhin *et al.*, 1999) were maintained on a mixed genetic background, including outcrosses to Swiss Black. Intercrosses were performed using *K14*-cre males and floxed hemizygous *Braf*^{V600E} females. Embryonic age, beginning at noon E0.5, was based on the day of post-coital plug detection. Animals were genotyped using primers in the study by Dankort *et al.*, (2007). Wild-type littermates were used as controls. Expression of *Braf* in wild-type and *Braf*^{V600E} mice is shown in Supplementary Figure S4 online. All experiments were performed and approved according to the institutional

guidelines established by the University of California, San Diego, Institutional Animal Care and Use Committee.

Assays for barrier function

Embryos were collected from E15.5 to E17.5. Dye exclusion assays were performed as essentially as described (Hardman *et al.*, 1998). Briefly, embryos were transferred through a methanol gradient and stained in 1% toluidine blue for 10 minutes and destained. To isolate cornified sheets, frozen embryonic skin was thawed and treated with Dispase II (Roche, Rotkreuz, Switzerland) for 1 hour at 37C, trypsinized, washed, and isolated. Dark field images of cornified sheets were observed with Olympus MVX10 stereomicroscope.

Tissue collection, storage, and RNA extraction

Tissue for immunostaining and histology was fixed in 4% paraformaldehyde and stored at 4 °C or flash frozen in OCT. Isolated epidermal sheet was obtained from embryonic skins incubated with Dispase II (Roche) and separated from the underlying dermis. RNA was extracted from epidermal sheets that were placed in Trizol reagent (Invitrogen, Carlsbad, CA) and disrupted with 1 mm zirconia beads (BioSpec Products, Bartlesville, OK). Prior to use, RNA was treated with RNase-free DNase and further concentrated using a RNA Clean & Concentrator kit (Zymo Research, Irvine, CA).

Histology, immunofluorescence, *in situ* hybridization

For immunofluorescent staining, the primary and secondary antibodies used in this study are described in Supplementary Methods online. *In situ* hybridizations were performed essentially as described (Etchevers *et al.*, 2001). Riboprobes were generated using T7 or SP6-modified oligos (Supplementary Table S1 online) and amplified by PCR.

RNA analysis by real-time PCR and high-throughput sequencing

Primer sequences are detailed in Supplementary Table S3 online using Primer3 (Rozen and Skaletsky, 2000), and real-time qPCR performed with Maxima First Strand cDNA Synthesis and SYBR Green/ROX qPCR Kits (Thermo Fermentas, San Francisco, CA) in triplicate on a Lightcycler 480 (Roche). A comparative CT method was used for analysis using *Gapdh* or *Beta-actin* for mouse mRNAs (Schmittgen and Livak, 2008).

For RNA sequencing, total RNA was pooled from four wild-type and mutant E17.5 epidermal sheets. NuGEN Ovation RNASeq v1 was used to generate cDNA, fragment, end repair, and polyA-tail following the TruSeq (Illumina, San Diego, CA) protocol. Raw data were processed using BOWTIE, FASTX-Toolkit and aligned to the mouse genome (mm9) (Trapnell *et al.*, 2009). For assembly and quantification, Cufflinks (Trapnell *et al.*, 2012) were used and differentially expressed genes identified by Cufflinks were expressed as log2-fold changes of mean FPKM of mutant and wild-type RNAs. Benjamini-Hochberg-corrected *q*-values were reported in volcano plots. RNA-seq data will be accessioned at NCBI SRA Archive, SUB373241.

Explant assay and drug treatment

Explant cultures were performed as previously described with small modifications (Halprin *et al.*, 1979). In brief, embryonic skin was isolated, cut into 4×2 mm strips, placed on a gelatin-coated 10 μm Isopore membrane filter (Millipore, Temecula, CA), and floated over Dulbecco's Modified Eagle's medium, 10% fetal calf serum (Invitrogen), with antibiotics at 37 °C for 0–24 hours in 7% CO2. Explants were treated with vehicle, U0126 (Promega, Madison, WI), or PLX4720 (EMD Chemicals, Temecula, CA) solubilized in dimethyl sulfoxide (<0.2% final). RNA was isolated from samples as described above, except that the whole skin was used, and immunostained sections were obtained from fixed explant tissue. For pulse-chase studies, 50 μg BrdU g^{-1} was injected intraperitoneally in pregnant mice 2 hours prior to isolation of embryos. Explants were fixed for 1 hour, blocked in OCT, and 8 μm sections were cut, rehydrated with decreasing concentrations of ethanol, denatured in 4N HCl, neutralized, trypsinized, and inactivated. The tissues were stained with anti-BrdU (1:200; Sigma-Aldrich, St Louis, MO) with secondary detection using the MOM kit (Vector Laboratories, Burlingame, CA) and Strepavidin-Alexa 488 (Life Technologies, Carlsbad, CA).

Epidermal sheets prepared from Dispase II (Roche)–treated embryonic skin. For dissociation, epidermal sheets were further treated with Accutase (Chemicon, Temecula, CA/Millipore), inactivated, and placed in the same media and growth conditions as described above. Viability of epidermal sheets and keratinocytes was validated by the presence of active transcription assessed at the end of 24 hour culture with 2 hour actinomycin treatment.

CONFLICT OF INTEREST

The authors state no conflicts of interest.

ACKNOWLEDGMENTS

We thank M. McMahon, D. Dankort, and C. Jamora for generously sharing animals carrying the conditional *Braf*^{V600E} allele and *K14*-cre and C. Jamora and R. Gallo lab for contributing reagents and helpful discussions. We thank the UCSD Skin Genomics Core for RNA-seq analysis. Research reported in this publication was supported by the National Institute of Arthritis and Musculoskeletal and Skin Diseases of the National Institutes of Health under award number AR056667, the California Institute for Regenerative Medicine RN2-00908, Joseph A. Stirrup Skin Cancer Foundation, R. Hotto Transdermal Research and institutional funds for B.D.Y. The content is solely the responsibility of the authors and does not necessarily represent the official views of the National Institutes of Health or other supporters.

SUPPLEMENTARY MATERIAL

Supplementary material is linked to the online version of the paper at http://www.nature.com/jid

REFERENCES

Aoki Y, Niihori T, Narumi Y *et al.* (2008) The RAS/MAPK syndromes: novel roles of the RAS pathway in human genetic disorders. *Hum Mut* 29:992–1006

Bloethner S, Chen B, Hemminki K *et al.* (2005) Effect of common B-RAF and N-RAS mutations on global gene expression in melanoma cell lines. *Carcinogenesis* 26:1224–32

Bollag G, Hirth P, Tsai J *et al.* (2010) Clinical efficacy of a RAF inhibitor needs broad target blockade in BRAF-mutant melanoma. *Nature* 467:596–9

Caplan AI, Ordahl CP (1978) Irreversible gene repression model for control of development. *Science* 201:120–30

Chapman PB, Hauschild A, Robert C *et al.* (2011) Improved survival with vemurafenib in melanoma with BRAF V600E mutation. *N Engl J Med* 364:2507–16

Chen X, Mitsutake N, LaPerle K *et al.* (2009) Endogenous expression of Hras(G12V) induces developmental defects and neoplasms with copy number imbalances of the oncogene. *Proc Natl Acad Sci USA* 106: 7979–84

Chowaniec O, Jablonska S, Beutner EH *et al.* (1981) Earliest clinical and histological changes in psoriasis. *Dermatologica* 163:42–51

Dankort D, Filenova E, Collado M *et al.* (2007) A new mouse model to explore the initiation, progression, and therapy of BRAFV600E-induced lung tumors. *Genes Dev* 21:379–84

de Guzman Strong C, Conlan S, Deming CB *et al.* (2010) A milieu of regulatory elements in the epidermal differentiation complex syntenic block: implications for atopic dermatitis and psoriasis. *Hum Mol Genet* 19: 1453–60

Etchevers HC, Vincent C, Le Douarin NM *et al.* (2001) The cephalic neural crest provides pericytes and smooth muscle cells to all blood vessels of the face and forebrain. *Development* 128:1059–68

Gomez C, Chua W, Miremadi A *et al.* (2013) The Interfollicular Epidermis of Adult Mouse Tail Comprises Two Distinct Cell Lineages that Are Differentially Regulated by Wnt, Edaradd, and Lrig1. *Stem Cell Reports* 1:19–27

Groesser L, Herschberger E, Ruetten A *et al.* (2012) Postzygotic HRAS and KRAS mutations cause nevus sebaceous and Schimmelpenning syndrome. *Nat Genet* 44:783–7

Hafner C, Groesser L (2013) Mosaic RASopathies. *Cell Cycle* 12:43–50

Halprin KM, Lueder M, Fusenig NE (1979) Growth and differentiation of postembryonic mouse epidermal cells in explant cultures. *J Invest Dermatol* 72:88–98

Hardman MJ, Sisi P, Banbury DN *et al.* (1998) Patterned acquisition of skin barrier function during development. *Development* 125:1541–52

Kakumoto K, Sasai K, Sukezane T *et al.* (2006) FRA1 is a determinant for the difference in RAS-induced transformation between human and rat fibroblasts. *Proc Natl Acad Sci USA* 103:5490–5

Koster MI, Roop DR (2007) Mechanisms regulating epithelial stratification. *Annu Rev Cell Dev Biol* 23:93–113

Lanzavecchia A, Sallusto F (2002) Progressive differentiation and selection of the fittest in the immune response. *Nat Rev Immunol* 2:982–7

Levinsohn JL, Tian LC, Boyden LM *et al.* (2013) Whole-exome sequencing reveals somatic mutations in HRAS and KRAS, which cause nevus sebaceus. *J Invest Dermatol* 133:827–30

Liaw D, Marsh DJ, Li J *et al.* (1997) Germline mutations of the PTEN gene in Cowden disease, an inherited breast and thyroid cancer syndrome. *Nat Genet* 16:64–7

Lin P, Baldassare JJ, Voorhees JJ *et al.* (1999) Increased activation of Ras in psoriatic lesions. *Skin Pharmacol Appl Skin Physiol* 12:90–7

Lindhurst MJ, Sapp JC, Teer JK *et al.* (2011) A mosaic activating mutation in AKT1 associated with the Proteus syndrome. *N Engl J Med* 365:611–9

MacLean NaH, B. K. (1987) *Cell commitment and differentiation*. University Press: Cambridge, 247

Mannik J, Alzayady K, Ghazizadeh S (2010) Regeneration of multilineage skin epithelia by differentiated keratinocytes. *J Invest Dermatol* 130:388–97

Morrison SJ, Shah NM, Anderson DJ (1997) Regulatory mechanisms in stem cell biology. *Cell* 88:287–98

Mukhopadhyay A, Krishnaswami SR, Cowing-Zitron C *et al.* (2012) Negative regulation of Shh levels by Kras and Fgfr2 during hair follicle development. *Dev Biol* 373:373–82

Mukhopadhyay A, Krishnaswami SR, Yu BD (2011) Activated Kras alters epidermal homeostasis of mouse skin, resulting in redundant skin and defective hair cycling. *J Invest Dermatol* 131:311–9

Muto S, Katsuki M, Horie S (2006) Rapid induction of skin tumors in human but not mouse c-Ha-ras proto-oncogene transgenic mice by chemical carcinogenesis. *Cancer Sci* 97:842–7

Okubo T, Clark C, Hogan BL (2009) Cell lineage mapping of taste bud cells and keratinocytes in the mouse tongue and soft palate. *Stem Cells* 27:442–50

Ortonne JP, Loning T, Schmitt D *et al.* (1981) Immunomorphological and ultrastructural aspects of keratinocyte migration in epidermal wound healing. *Virchows Arch A Pathol Anat Histol* 392:217–30

Patel GK, Wilson CH, Harding KG *et al.* (2006) Numerous keratinocyte subtypes involved in wound re-epithelialization. *J Invest Dermatol* 126: 497–502

Pilarski R, Burt R, Kohlman W *et al.* (2013) Cowden syndrome and the PTEN hamartoma tumor syndrome: systematic review and revised diagnostic criteria. *J Natl Cancer Inst* 105:1607–16

Poulikakos PI, Zhang C, Bollag G *et al.* (2010) RAF inhibitors transactivate RAF dimers and ERK signalling in cells with wild-type BRAF. *Nature* 464: 427–30

Rauen KA (2013) The RASopathies. *Annu Rev Genomics Hum Genet* 14: 355–69

Razzaque MA, Nishizawa T, Komoike Y *et al.* (2007) Germline gain-of-function mutations in RAF1 cause Noonan syndrome. *Nat Genet* 39: 1013–7

Roberts A, Allanson J, Jadico SK *et al.* (2006) The cardiofaciocutaneous syndrome. *J Med Genet* 43:833–42

Rodriguez-Viciana P, Tetsu O, Tidyman WE *et al.* (2006) Germline mutations in genes within the MAPK pathway cause cardio-facio-cutaneous syndrome. *Science* 311:1287–90

Rozen S, Skaletsky H (2000) Primer3 on the WWW for general users and for biologist programmers. *Methods Mol Biol* 132:365–86

Schmittgen TD, Livak KJ (2008) Analyzing real-time PCR data by the comparative C(T) method. *Nat Protoc* 3:1101–8

Schuhmacher AJ, Guerra C, Sauzeau V *et al.* (2008) A mouse model for Costello syndrome reveals an Ang II-mediated hypertensive condition. *J Clin Invest* 118:2169–79

Sebolt-Leopold JS (2008) Advances in the development of cancer therapeutics directed against the RAS-mitogen-activated protein kinase pathway. *Clin Cancer Res* 14:3651–6

Sengel P (1976) *Morphogenesis of Skin*. Cambridge University Press: UK, 277

Siegel DH, McKenzie J, Frieden IJ *et al.* (2011) Dermatological findings in 61 mutation-positive individuals with cardiofaciocutaneous syndrome. *Br J Dermatol* 164:521–9

Sosnowski RG, Feldman S, Feramisco JR (1993) Interference with endogenous ras function inhibits cellular responses to wounding. *J Cell Biol* 121:113–9

Spivakov M, Fisher AG (2007) Epigenetic signatures of stem-cell identity. *Nat Rev Genet* 8:263–71

Tarutani M, Cai T, Dajee M *et al.* (2003) Inducible activation of Ras and Raf in adult epidermis. *Cancer Res* 63:319–23

Trapnell C, Pachter L, Salzberg SL (2009) TopHat: discovering splice junctions with RNA-Seq. *Bioinformatics* 25:1105–11

Trapnell C, Roberts A, Goff L *et al.* (2012) Differential gene and transcript expression analysis of RNA-seq experiments with TopHat and Cufflinks. *Nat Protoc* 7:562–78

Tsai J, Lee JT, Wang W *et al.* (2008) Discovery of a selective inhibitor of oncogenic B-Raf kinase with potent antimelanoma activity. *Proc Natl Acad Sci USA* 105:3041–6

Turnpenny PD, Dean JC, Auchterlonie IA *et al.* (1992) Cardiofacio-cutaneous syndrome with new ectodermal manifestations. *J Med Genet* 29:428–9

Urosevic J, Sauzeau V, Soto-Montenegro ML *et al.* (2011) Constitutive activation of B-Raf in the mouse germ line provides a model for human cardio-facio-cutaneous syndrome. *Proc Natl Acad Sci USA* 108: 5015–20

Vasioukhin V, Degenstein L, Wise B *et al.* (1999) The magical touch: genome targeting in epidermal stem cells induced by tamoxifen application to mouse skin. *Proc Natl Acad SciUSA* 96:8551–6

Vassar R, Fuchs E (1991) Transgenic mice provide new insights into the role of TGF-alpha during epidermal development and differentiation. *Genes Dev* 5:714–27